NMR Study of Si:As and Si:P near the metal-insulator transition

M. J. Hirsch and D. F. Holcomb
Laboratory of Atomic and Solid State Physics, Cornell University, Ithaca, New York 14853-2501
(Received 30 September 1985)

Results of pulsed NMR measurements on the ^{29}Si spin system in Si:As and Si:P are reported for samples spanning the metal-insulator (*M-I*) transition. The ranges of donor concentrations n_D are 1.6×10^{18} to 4×10^{19} cm^{-3} for Si:As and 1.1×10^{17} to 6.9×10^{19} cm^{-3} for Si:P. The measurements, made at 4.3 K and primarily in a resonant field of 58.5 kG, show that nonzero values of peak Knight shifts and a Korringa-like spin relaxation are observed for values of n_D/n_c as low as 0.4. Knight-shift distributions for Si:As and Si:P at a given value of n_D appear to coincide at values of n_D near 10^{20} cm^{-3}, but differ near the respective critical concentrations for the two systems. Values of local Knight shifts change smoothly through the *M-I* transition. Knight-shift distributions determine the inhomogeneous linewidth. Spin-echo measurements give a determination of the homogeneous, dipolar width. The nuclear spin system does not relax with a single value of T_1. Interpretation of the data emphasizes the importance of focusing attention on the distribution of values of Knight shift and T_1 in this disordered system, rather than attempting to characterize the system with a single value of K or T_1.

I. INTRODUCTION

Recent measurements of electrical transport properties near the metal-insulator (*M-I*) transition in *n*-type silicon have given a rather complete picture of electron localization processes in Si:P (Ref. 1) and, with less detail, in Si:As.[2,3] Although there remain some unanswered questions with respect to the best theoretical model to use to describe the transition,[1] the broad outlines of the necessary theory are rather clearly defined.

In this paper, we are primarily concerned with magnetic properties. The work of Andres *et al.*[4] and the scaling model of Bhatt and Lee[5] seem to give a generally satisfactory picture of the concentration and temperature dependence of the magnetic susceptibility on the insulating side of the transition. On the metallic side, the situation is much less clear. Although Quirt and Marko[6] were able to fit the temperature dependence of their low-field spin susceptibility data in Si:P very well with a phenomenological model based on a separation into a "Pauli component" and a "Curie-Weiss component," the physical origin of the Curie-Weiss component has remained obscure. Moreover, the concentration dependence of the ^{29}Si NMR Knight shift near the transition has remained only very sketchily interpreted.[7,8]

The purpose of the experiments reported here was to carefully study the evolution of line shapes and values of Knight shift as the metal-insulator transition was traversed by changing donor concentration n_D. Some data concerning relaxation time behavior are also given.

The most complete report of previous measurements of ^{29}Si NMR properties for Si:P was given by Kobayashi, Fukagawa, Ikehata, and Sasaki (hereinafter abbreviated as KFIS) in Ref. 8. In general, the KFIS results are consistent with a picture in which the various magnetic properties change smoothly across the *M-I* transition, while other properties governed by the electron system, such as dielectric polarizability[9,10] and dc electrical conductivity,[1] are exhibiting critical behavior. Our measurements extend those of KFIS in several ways. (i) We have studied Si:As as well as Si:P. (ii) We have measured values of Knight shift K and linewidth at a resonance field of 58.5 kG, rather than the 9.1 kG used by KFIS. We have also made linewidth measurements on Si:As samples at both 58.5 and 10 kG. (iii) The better signal-to-noise and higher resolution available at 58.5 kG permit accurate measurements of Knight shifts for samples below the *M-I* transition for the first time. Our results provide a more complete picture of the slow evolution of the NMR properties as the donor concentration decreases through the *M-I* transition. In particular, the basic features of the Korringa model[11] of Knight shift and nuclear-spin relaxation behavior remain intact for values of n_D well below n_c, the value of n_D at the *M-I* transition. This result implies the existence of a near continuum of electron states (which are localized, in the charge-transport sense) at the Fermi level. Our analysis seems quite consistent with results of the careful study of a sample of Si:P at $n_D=2.5\times10^{18}$ cm^{-3} by Jerome, Ryter, and Winter[12] some years ago, and with a recent reexamination of the results of that study.[13] We note the importance of keeping in mind that NMR experiments are sensitive to *local* properties of the electron-spin system. In the doped semiconductor systems, the random distribution of impurities causes these local properties to vary from site to site. Although, for convenience, we may refer from time to time to "the Knight shift" or "the relaxation rate," there is, in fact, a distribution of both of these characteristic NMR parameters.

We note that the behavior of the Knight shift and relaxation time of the ^{29}Si spin system in the heavily doped semiconductors, in samples with donor concentration below the *M-I* transition, appears to have much in common with the results of similar studies[14] in a doped and compensated tungsten oxide system $Na_xTa_yW_{1-y}O_3$.

Some of our results and interpretation are at variance with those of KFIS, and we shall call attention to those at an appropriate time. All of our measurements were made at a temperature of 4.3 K and are, thus, so far removed from the domain of the low-field and low-temperature measurements recently reported by Palaanen, Ruckenstein, and Thomas[15] that the two studies may speak to rather different aspects of the NMR (and electronic) behavior.

II. EXPERIMENTAL DETAILS

Our samples (see Table I) came from a variety of sources. The three Si:P samples with the lowest phosphorus concentration, P1, P2, and P3, were made from the crystals supplied by Allegheny Electronic Chemicals Co. (now Pensilco) which were used by Sundfors and Holcomb.[7] The three samples with the highest phosphorus concentration, P6, P5, and P4, were used by Brown and Holcomb.[16] The room-temperature resistivities of these samples were known, and by using the calibration curve of Thurber, Mattis, Liu, and Filliben,[17] the phosphorus concentration could be determined. Due to a range of measured resistivity values for a given sample, the phosphorus concentration is uncertain to $\pm 10\%$.

The arsenic samples were prepared from wafers sliced from melt-grown single crystals of Si:As. These wafers were typically 0.4 mm thick and 5 cm in diameter. Resistivities across a wafer diameter were measured with an in-line four-point probe with nominal tip spacing of 0.16 cm. The resistivity values had cylindrical symmetry about the center of the wafer. A calibration curve for Si:As (Ref. 18) was used to convert resistivities to arsenic concentration. This calibration curve, however, is only valid up to arsenic concentrations of 1.1×10^{19} cm^{-3}. Samples A9 and A8 had concentrations which were outside the range of validity of the Si:As calibration curve. To determine their concentration, we measured the Hall constant R_H at room temperature and used the relation $n_D = A/R_H e$. The value of the Hall scattering factor A was estimated to be 1.2. This estimate is based on some preliminary measurements we have made using neutron activation techniques to determine absolute donor concentrations of Si:As samples at values of n_D higher than those reported in Ref. 18. Samples of Si:As were more homogeneous than the Si:P samples. The concentration variation of a single arsenic sample was typically $\pm 2\%$, while the absolute uncertainty in average concentration arising from uncertainties in the Si:As calibration curve is $\pm 4\%$. For samples A8 and A9, we estimate the uncertainty in the derived value of n_D to be $\pm 15\%$.

To fabricate the NMR samples, 2.5-cm-diam disks were ultrasonically cut from the center of the wafers. These disks were then crushed to grain sizes ranging from 100 to 1000 μm, depending on the electrical conductivity of the sample. In all cases, the grain dimensions were at least a factor of 3 smaller than the skin depth at 50 MHz. This skin depth is typically 1 mm for the range of conductivities of our samples. The crushed powders were cast in paraffin in cylindrical molds. The cylindrical samples were 1 cm long and 0.6 cm in diameter, and fit snugly into a NMR coil.

The pulsed NMR spectrometer is based on a design by Gordon,[19] which was, in turn, based on the design of Ellett *et al.*[20] It is a superheterodyne system and uses an intermediate frequency of 160 MHz. Phase-sensitive detection is used, and the audio output is brought out on two channels, 90° out of phase. Availability of these quadrature outputs simplifies the process of obtaining the Fourier transform of the signal. Each audio channel has a two-pole active Bessel filter at its output. The Bessel configuration is particularly suitable for pulsed NMR experiments. By shifting the phase of each frequency component by an amount proportional to its frequency, it introduces less distortion of a single in the time domain then, e.g., a Butterworth or Chebyshev filter with the same upper cutoff frequency. The audio bandwidth was set at 30 kHz. This bandwidth produces some distortion of the initial part of the free induction decay (FID), which

TABLE I. Properties of samples of Si:As and Si:P.

Sample	Donor impurity	ρ295 (mΩ cm)	Donor concentration n_D(cm^{-3})	Knight shift at 58.5 kG Peak	Knight shift at 58.5 kG K_{cg}	FWHM linewidth (G) 58.5 kG	FWHM linewidth (G) 10 kG
A1	As	18.0	1.6×10^{18}	0	8.6×10^{-6}	0.6	0.21
A2	As	12.2	3.6×10^{18}	5.8×10^{-6}	1.9×10^{-5}	1.16	
A3	As	7.94	8.0×10^{18}	9.4×10^{-6}	2.8×10^{-5}	1.63	
A4	As	7.77	8.3				0.37
A5	As	7.47	8.8×10^{18}				0.44
A6	As	7.24	9.2×10^{18}				0.45
A7	As	6.47	1.08×10^{19}	1.35×10^{-5}	4.3×10^{-5}	1.86	0.41
A8	As	2.27	4.0×10^{19}				0.81
A9	As	2.27	4.0×10^{19}	3.5×10^{-5}	6.6×10^{-5}	3.72	
P1	P	80	1.1×10^{17}	0		0.5	
P2	P	15.1	2.2×10^{18}	4.6×10^{-6}	1.7×10^{-5}	0.79	
P3	P	9.0	5.4×10^{18}	1.2×10^{-5}	3.7×10^{-5}	1.8	
P4	P	3.67	1.8×10^{19}	2.5×10^{-5}	5.5×10^{-5}	2.98	
P5	P	2.36	2.9×10^{19}	3.66×10^{-5}	6.2×10^{-5}	3.63	
P6	P	1.06	6.9×10^{19}	6.35×10^{-5}	9.5×10^{-5}	5.23	
SB1	Sb	11.4	3.7×10^{18}			1.4	

contains many high-frequency Fourier components.[21] This distortion fades away after a time following the end of the pulse equal to the reciprocal of the bandwidth. This time interval of 30 μsec, during which information was unavailable, was short compared with the shortest FID we recorded, about 300 μsec. The length of radio-frequency pulse needed to tip the Si magnetization by 90° was 9 μsec. This pulse length corresponds to a value of the oscillating magnetic field in the coil H_1 of 33 G.

The two quadrature signals from the receiver were recorded on a Nicolet 4094 digital oscilloscope, which digitizes at a maximum rate of 2 MHz. A Fourier transform of the FID was performed on a general purpose PRIME computer which serves experimental groups in our laboratory. When taking a Fourier transform, there is a phase parameter which determines the mixture of absorptive and dispersive components in the result. The NMR line shape is the absorptive part of the spectrum. To ensure that we did not mix in any dispersive component, we adjusted the phase to maximize the ratio A/B, where A is the area of the transform above the base line and B is the area below the base line.

Our external field was generated by an Oxford superconducting solenoid operating in the persistent mode. The value of the field for most of our measurements was 58.5 kG, which set our rf frequency at 49.5 MHz. The inhomogeneity of the field over the sample volume was measured to be 50 mG, a factor of 10 smaller than the narrowest line which we measured. The magnetic field for the 10-kG measurements was provided by a Walker electromagnet. Its inhomogeneity over the sample volume was 35 mG.

One of our goals in these experiments was to obtain the highest possible precision in the measurement of the very small values of K which are found in samples with donor concentrations near and below the M-I transition. Even though the Oxford solenoid meets its specifications with respect to an average rate of drift of the resonance field, we found the drift rate quite nonuniform. Occasionally, the field changes quickly with a typical magnitude of a few tenths of a gauss. For our samples, the spin-lattice relaxation time T_1 is typically an hour or two. We needed to keep the time interval between measurement of an experimental sample and of a reference sample short, to minimize the possibility of a small field shift occurring within that interval. This was done by constructing a probe which held two samples, each with its own coil and rf coax line. A 180° rotation of the probe would interchange the positions of the samples in the external field. With this scheme, both a sample of interest and a reference sample could be polarized in the external field during the same time interval. When both samples had polarized, the FID from one of them was recorded, the probe was rotated by 180°, and then the FID of the other was recorded. The time between the two FID recordings was typically three minutes. This double sample probe was constructed so that the value of the oscillating field produced in one coil due to a rf pulse in the other coil was roughly a factor of 400 smaller than the value of H_1 in the coil which was pulsed.

Our Knight-shift measurements used a Si:As reference sample with $n_D = 1.6\times10^{18}$ cm^{-3}. We checked this reference sample against a very lightly doped sample of Si:P, with $n_D = 1.1 = 10^{17}$ cm^{-3}. To within experimental error, these samples had the same resonance frequency. The Si:As sample was subsequently used as a Knight-shift reference because of its shorter value of T_1.

III. KNIGHT-SHIFT DISTRIBUTION

A. Experimental data

Figure 1 shows a typical NMR absorption line shape, obtained for sample A7. The NMR lines for all samples in Table I, obtained by taking the Fourier transform of the FID which follows a single 90° pulse, were found to be inhomogeneously broadened. (Measurements and analysis of the homogeneous line are treated in the Appendix.) In a disordered system, each nuclear site will, in general, have a different value of the local magnetic field. The asymmetric line reflects the distribution of local fields in the sample. In Fig. 1, one notes that the high-frequency side of the line has a long tail, indicating a large spread in the distribution of positive Knight shifts. Samples with lower donor concentration, while exhibiting narrower lines, showed the same type of asymmetry as the more metallic samples. Even our lowest concentration sample P1 had a slightly asymmetric line shape.

In describing and analyzing line shape data, we use three parameters indicated in Fig. 1. They are (i) the value of K at the peak of the absorption line, K_{pk}; (ii) the value of K at the center of gravity of the line, K_{cg}; and (ii) ΔH, the full width of the resonance line at half maximum intensity.

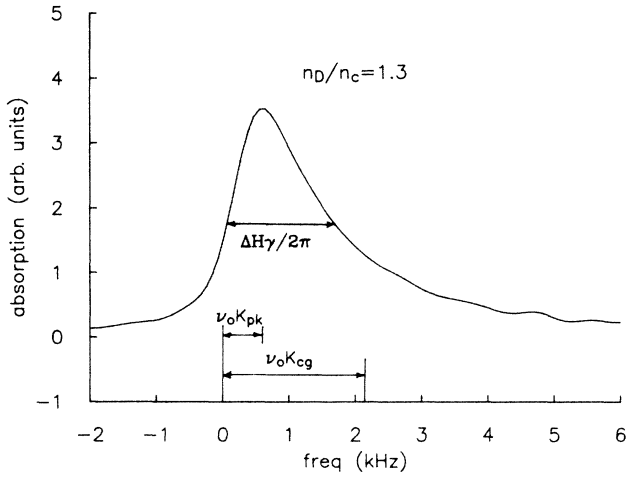

FIG. 1. Line shape for ^{29}Si in Si:As, sample A7, obtained by performing a Fourier transform of the free induction decay following a 90° pulse. The resonance position of our Knight-shift reference sample is at 0 kHz. The line shape shown is both broadened and shifted to higher frequencies by the distribution of Knight shifts in the sample. The width of the line in frequency units is related to the width in gauss by $\Delta\nu = (\gamma/2\pi)\Delta H$. The shift in frequency of either the peak position or the center of gravity, divided by the resonance frequency ν_0 of 49.5 MHz, gives a measure of the Knight-shift distribution.

Our results for K_{pk} in Si:P, measured in an external field of 58.5 kG, are shown in Fig. 2, along with the KFIS data for K_{pk}, taken at $H_0=9.1$ kG. Also shown are the spin susceptibility data of Quirt and Marko,[6,22] measured at $H_0=3.2$ kG. We note that our data merge with the KFIS results at high donor concentrations, show a much more gradual drop in K_{pk} near the M-I transition[1] at $n_D=3.74\times10^{18}$ cm^{-3} than the data of KFIS, and show $K_{pk}>0$ for values of n_D below n_c. We have extended these measurements to Si:As. In Fig. 3, we plot data for K_{pk} obtained for donor concentrations on both sides of the M-I transition for both Si:P and Si:As.

The data in Fig. 3 suggest that the Si:P and Si:As curves merge for absolute donor concentrations above 10^{20} cm^{-3}. For low concentrations, below roughly 2×10^{18} cm^{-3}, the curves for the two systems may again come together. But in the concentration region containing the critical concentrations for the two systems, the Knight-shift curves separate at a given concentration. For both the Si:P and Si:As curves, there is a region of larger slope which includes the respective M-I transitions, 3.74×10^{18} cm^{-3} for Si:P and 8.5×10^{18} cm^{-3} for Si:As.[2] At the critical concentrations, K_{pk} is nearly the same for both systems, with a value of 1×10^{-5}.

In analyzing the width of the Si NMR absorption line ΔH, we wish to focus on that contribution to the width which is due to the effects of impurity doping. There is a background width of 70 mG with a roughly Lorentzian shape which arises from the ^{29}Si-^{29}Si dipolar interaction (see the Appendix for a discussion of this dipolar width). In addition, there is a width due to magnet inhomogeneity of about 50 mG. One would not expect this magnet width to have the long tails associated with a Lorentzian line. Thus, we use the number 100 mG as a reasonable estimate of a correction to be subtracted from the total observed linewidth. The reduced linewidth, $\Delta H^*=\Delta H-0.10$ G, measures the spread in values of K.

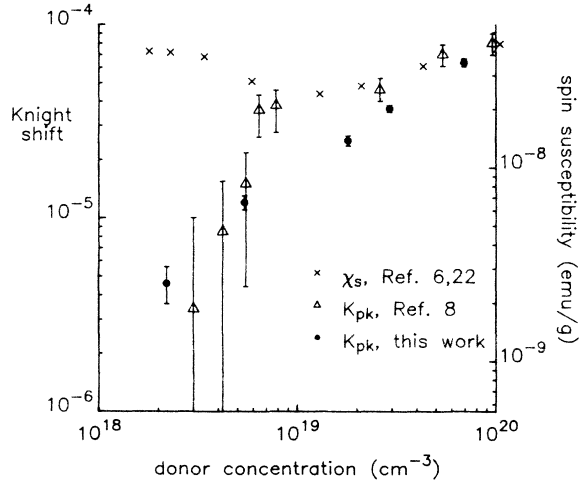

FIG. 2. A comparison of our peak Knight-shift data for Si:P in a field of 58.5 kG with the earlier Si:P data of Ref. 8, which was taken in a field of 9.1 kG. We also plot the spin susceptibility data of Refs. 6 and 22. The right-hand ordinate scale gives units of susceptibility, with the scale shifted so that K_{pf} and χ_s coincide at $n_D=10^{20}$ cm^{-3}.

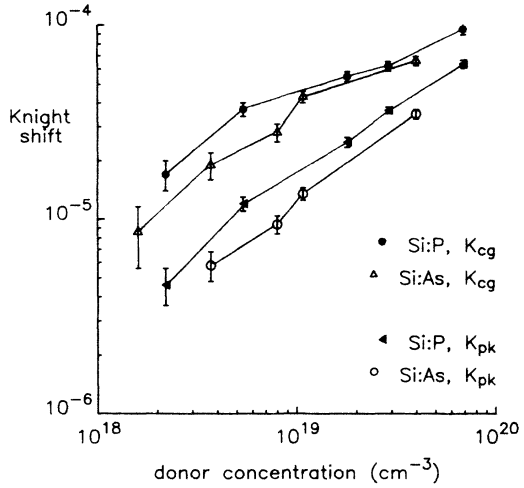

FIG. 3. Knight-shift data at $H_0=58.5$ kG for Si:As and Si:P as a function of donor concentration n_D. K_{pk} and K_{cg} are defined in Fig. 1.

The variation of ΔH^* with donor concentration is shown in Fig. 4. We have normalized all linewidths by dividing by 58.5 kG. The similarities between this figure and Fig. 3 are obvious. Again the Si:P and Si:As curves merge at high and low concentrations, with a splitting in the critical region. The linewidth at the critical concentration is the same for both Si:P and Si:As. The value of the linewidth is also roughly equal to the shift in resonance field, $K_{pk}H_0$, due to the Knight shift. It seems clear that the linewidth of these asymmetric lines is, in fact, due to the distribution of Knight shifts, for samples both above and below the M-I transition.
for samples both above and below the M-I transition.

Also included in Fig. 4 is a single data point for a sample of Si:Sb with the same donor concentration as one of the Si:As samples. The Si:Sb system[23] has a critical concentration n_c of 2.9×10^{18} cm^{-3}. Thus, the Si:Sb sample

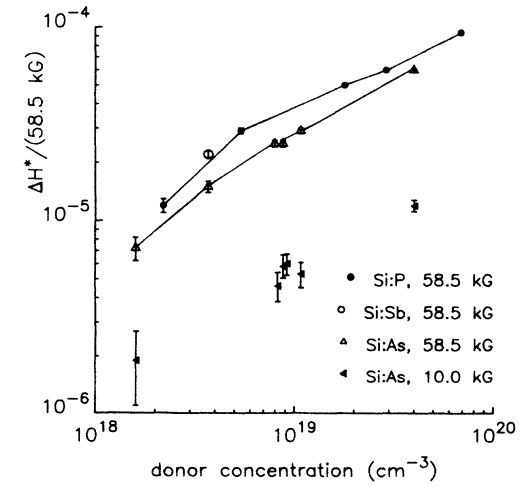

FIG. 4. Normalized ^{29}Si linewidth $\Delta H^*/(58.5$ kG), as a function of donor concentration for Si:As and Si:P. A single point for Si:Sb is also plotted. Data for Si:As at $H_0=10$ kG are shown.

has $n_D > n_c$, while the Si:As sample with the same donor concentration is well below the M-I transition point in Si:As. The difference in concentration relative to the respective critical concentration is reflected in the fact that ΔH^* for Si:Sb is larger than ΔH^* for the Si:As sample. This difference is consistent with the comparison of Si:P and Si:As, namely, that for donor concentrations near n_c the Si:P curve lies above the Si:As curve.

B. Analytical models

Many of our interpretations and conclusions depend upon an examination of the distribution of local magnetic fields seen by the various ^{29}Si nuclei which contribute to the NMR signal. These local fields provide a probe for the behavior of the electron-spin susceptibility χ_s, through the intermediary of the hyperfine interaction, $A\mathbf{I}\cdot\mathbf{S}$, where $\mathbf{I}$ is the nuclear spin and $\mathbf{S}$ the electron spin. In the basic, noninteracting electron, Korringa model,[11] the resonance field shift can be written as

$$K=\frac{\Delta\omega}{\omega_0}=\frac{8\pi}{3}\langle|u(0)|^2\rangle_{E_F}\chi_s\ , \tag{1}$$

where $\langle|u(0)|^2\rangle_{E_F}$ is the square of the electron wave function at the nuclear site averaged over electron states on the Fermi surface and χ_s is the electron-spin susceptibility.

In systems such as ours, with a broad distribution of local environments seen by the Si nuclei as a consequence of the random placement of the impurity atoms P or As, we need to modify the homogeneous form of Eq. (1). A useful form is given as

$$K_i=8\pi/3\langle|u(r_i)|^2\rangle E_F N_{\rm loc}\frac{\gamma_e\hbar}{H_0}\langle S_z\rangle\ . \tag{2}$$

$N_{\rm loc}$ is the local electron density averaged over a suitably chosen sampling volume. $\langle S_z\rangle$ is the value of the component of $\mathbf{S}$ parallel to the external field, again averaged over a suitably chosen sampling volume. This equation gives an expression for the value of the Knight shift at a particular ^{29}Si site position r_i. We have broken up the expression for spin susceptibility by writing it in the form

$$\chi_s=N_{\rm loc}\frac{\gamma_e\hbar}{H_0}\langle S_z\rangle\ .$$

ESR experiments[24] show strong exchange interactions between impurity electron spins in the concentration range of interest, $n_D > 10^{18}$ cm^{-3}. Thus, we believe it reasonable to assume that $\langle S_z\rangle$ is not a local property, but has the same value at all points because of the rapid spin exchange. Our model requires that the characteristic diameter of the sampling volume for $N_{\rm loc}$ be large compared to the interimpurity spacing, so that many impurity sites contribute an electron to the electron distribution sampled by the ^{29}Si nucleus in question. The wave-function factor $\langle|u(r_i)|^2\rangle E_F$, which we represent subsequently by the simplified symbol P_i, is expected to vary from site to site, as a consequence of the degree of proximity of that site to one or more donor ions. We note that the average over states at the Fermi surface, which includes the full electron distribution in an ordered metal, may now be restricted to a smaller number of states—those whose wave functions have nonzero amplitudes at the Si site in question.

According to the model represented by Eq. (2), our resonance line shapes, such as those shown in Fig. 1, are plots of the probability of various values of the product $P_i N_{\rm loc}$ for a sample with a given value of $\langle S_z\rangle$.

C. Discussion

1. *Spin susceptibility and K for $n_D \gg n_c$*

Changes in any of the magnetic properties as n_D is varied through the M-I transition are small when compared to changes in the transport properties. From Fig. 3 we see that values of $K_{\rm pk}$ in the concentration range from 1.0×10^{18} cm^{-3} to 7×10^{19} cm^{-3} increase smoothly as n_D is increased, very roughly following the power law $K_{\rm pk}\propto n^{0.7}$ for both systems.

Some rather simple considerations explain the fact that the Si:P and Si:As values of $K_{\rm pk}$ shown in Fig. 3 appear to merge as n_D approaches 10^{20} cm^{-3}. At concentrations much greater than n_c, the donor atom potentials are so heavily overlapped that the wave functions spread rather uniformly through the system and are insensitive to the minor differences in the central-cell potential from one donor to another. There remains a statistical distribution of values of $N_{\rm loc}$ and P_i, and the broad, asymmetric line is still seen. But the typical wave function is now spread through the Si lattice, rather than being strongly peaked near a donor core. In Figs. 2 and 3 we note that in our data, the condition $K_{\rm pk}\propto\chi_s\propto n^{1/3}$ is only reached as n_D nears 10^{20} cm^{-3}. The KFIS data, at $H_0=9.1$ kG, show this proportionality as appearing at a somewhat lower value of n_D, about 3×10^{19} cm^{-3}.

2. *Knight-shift distribution for n_D near and below n_c*

For n_D near and below n_c, the Knight shift should not necessarily be independent of the type of donor, since the localized states have different spatial distributions for different donors. In the simplest model, the Bohr radii of hydrogenlike states for P and As will be related to the isolated donor ionization energies (45.3 meV for Si:P and 53.5 meV for Si:As).[25] Taking the Bohr radius for P to be 17.3 Å,[26] we calculate the Bohr radius for As to be 14.6 Å. Although data points are sparse, it seems clear in Fig. 3 that the curves for Si:P and Si:As separate in the region which includes their respective values of n_c, with a region of steeper slope for both near the M-I transition. This increase in slope of the $K_{\rm pk}$ versus n_D curve near $n_D=n_c$ is qualitatively similar to the steep falloff seen in the KFIS data, although the feature in our data is a muted version. We shall return later to a discussion of the differences in our data and those of KFIS. For the moment, we consider the rather striking feature (remarked upon by previous workers) that values of $K_{\rm pk}$ or $K_{\rm cg}$ drop sharply away from the proportionality to χ_s which is observed for $n_D \gg n_c$ and which is suggested by Eq. (1) for a simple, homogeneous metal. Because this drop in values of K, also seen in Ge:As,[27] occurs near n_c, it has been natural to try to relate it to the carrier localization phenomenon of

the M-I transition. However, no detailed model expressed in these terms yet exists.

While we also have no detailed model, we will argue that the departure from the condition $K_{pk} \propto \chi_s$ which appears as n_D drops near n_c is a natural consequence of a transition from the high-density limit, where donor core potentials are strongly overlapped and every ^{29}Si nucleus is in the field of influence of many donors, to a low-density limit in which the local hyperfine field at a ^{29}Si site is governed primarily by its position in a roughly exponential electron wave function centered on the nearest donor site.

Consider the high-density limit. The condition $K_{pk} \propto \chi_s$ will result if the distribution of values of P_i is independent of n_D. That will be the case only when the donor cores are so heavily screened that most ^{29}Si nuclei find themselves in a region of rather uniform background potential. As the density is lowered, the Thomas-Fermi screening length $1/q$ increases. As the screening length increases, the potential distribution becomes lumpier, and the wave functions peak strongly near the donor cores. This wave-function concentration near the cores (where a relatively small number of ^{29}Si nuclei reside) automatically reduces the probability density in the region far from the cores. This open space in between the donor cores includes a much larger fraction of the ^{29}Si nuclei. Thus, the local Knight shifts of the majority of the nuclei are reduced by this concentration of electron wave functions near the cores.

In attempting to estimate the value of $1/q$ at which a crossover from the high-density limit to the low-density limit might becomes visible, it is natural to compare the screening length to the effective Bohr radius of the isolated donor a_H^*. Mott[28] argued that the critical value of the screening for the M-I transition would be reached when $1/q = a_H^*$. We expect the change from rather uniformly spread wave functions to strongly peaked wave functions to develop at roughly the same value of $1/q$, even though that change does not depend in any direct way on the conductivity transition.

This line of argument naturally differentiates between Si:P and Si:As. Because of the smaller value of a_H^* for Si:As, K_{pk} will drop away from the condition $K_{pk} \propto \chi_s$ at a higher value of n_D. Table II shows that $1/q$ crosses the value a_H^* at about 2×10^{19} cm^{-3} for Si:As and at about 9×10^{18} cm^{-3} for Si:P. The ratio of these numbers is roughly equal to the ratio of the values of n_D at which the slope of the K_p versus n_D curve has its maximum value for Si:As and Si:P, respectively, (see Fig. 3).

It is interesting to speculate on the relationship between the distribution of K values represented by the NMR absorption line of sample P2, with $n_D = 2.2\times10^{18}$ cm^{-3}, and those determined for ^{29}Si nuclei very near the P impurity cores by Jerome *et al.*[12] in a sample with $n_D = 2.5\times10^{19}$ cm^{-3}. For sample P2, $K_{pk} = 4.6\times10^{-6}$. The long tail to high values of K has measurable amplitude at $K = 5\times10^{-5}$. The Jerome *et al.* experiments see values of K from 8×10^{-4} to 7×10^{-3} (at 1.3 K) for that small fraction of nuclei very near the P impurities. There is every reason to expect that there is a continuous distribution of values of K in the spectral region between the two measurements, values not visible in our experiment because of signal-to-noise considerations.

TABLE II. Values of Thomas-Fermi screening length, r_{TF}, for various electron concentrations in silicon.

n_D (cm^{-3})	$1/q$[a] (Å)
2.3×10^{18}	21.7
5×10^{18}	19.1
1.0×10^{19}	16.9
2.0×10^{19}	14.6

[a] $1/q = [\hbar^2\kappa/4m^*e^2(3n/\pi)^{1/3}]^{1/2}$, where n is the electron density, κ is the dielectric constant (12 for Si), and m^* is the conductivity effective mass. For Si, $m^* = 0.26m_0$.

3. *Comparison of our data with that of KFIS*

The difference between our data for Si:P and that of KFIS, seen in Fig. 2 in the concentration range 6×10^{18} cm$^{-3} < n_D < 3\times10^{19}$ cm^{-3}, might reasonably be ascribed to the fact that the applied static field differs by a factor of 6. However, examination of our linewidth data shows that an apparent inconsistency does exist. A comparison of Figs. 3 and 4 strongly suggests that at $H_0 = 58.5$ kG, the linewidth arises from a distribution of local values of K. Both the concentration dependences and the magnitudes of the field shift and widths are very similar.

The linewidth plot resembles the Knight-shift plot even more closely if instead of the peak Knight shift one plots the center-of-gravity Knight shift

$$K_{cg} = \int \omega f(\omega) d\omega \Big/ \int f(\omega) d\omega \ .$$

Here, $f(\omega)$ is the line-shape function and $\omega = 0$ is the zero Knight-shift position. The plot of K_{cg} versus n_D is also shown in Fig. 3. Up until this point, we have emphasized K_{pk} rather than K_{cg} because K_{pk} can be more precisely determined experimentally. (K_{cg} is the first moment of the line shape, with respect to the $K=0$ reference position, and is sensitive to the exact shape and degree of asymmetry of the line. But the tails of the line are often difficult to measure accurately. Thus, K_{cg} has larger error bars than K_{pk}.)

Since the distribution of Knight shifts is responsible for the linewidth, we expect the concentration dependence of the Knight shifts and the linewidth to be the same. A comparison of the linewidth data at two field strengths, 10 kG and 58.5 kG, in Fig. 4, shows a common concentration dependence. This common dependence would seem to rule out any concentration-dependent susceptibility saturation effect in going from 10 to 58.5 kG. We are logically led to the conclusion that the Knight-shift curves at 10 and 58.5 kG should have similar shapes. But the KFIS Knight-shift data at 9.1 kG show a sharp drop as n_D is decreased through the transition, a drop seen in neither our linewidth data at 10 kG nor in or Knight-shift measurements at 58.5 kG. We can only speculate on the reason for this inconsistency until we repeat the low-field Knight-shift measurements.

One may wonder whether the shrinking of the electron

wave functions caused by the external field is responsible for the different characteristics of K at the two different values of field. One relevant parameter to consider is the magnetic length $\lambda=(\hbar c/eH)^{1/2}$, which is the radius of an electron orbit in the first Landau level of a system in a magnetic field. For $H=58.5$ kG, λ has a value of 100 Å. Magnetic field effects should become important when this length becomes comparable to or shorter than other length scales in the problem. For the Si:P system, the donor Bohr radius is 17 Å, while a measure of the distance between impurities, $n_D^{-1/3}$, is 46 Å at $n_D=1\times10^{19}$ cm^{-3}. The correlation length ξ which characterizes the long-wavelength modulation of the electron wave function above the M-I transition is large only for donor concentrations close to the critical concentration n_c and at low temperatures in the millikelvin range. The zero-temperature expression for ξ is[29]

$$\xi=\xi_0\,|\,(n-n_c)/n_c\,|^{-\nu},$$

where ξ_0 is the order of the Bohr radius and ν is 0.5.[1] The phosphorus sample closest to the M-I transition had $n_D=1.44n_c$, which leads to a zero-temperature coherence length of $\xi=1.53\xi_0$. The coherence length at finite temperatures will be smaller, due to thermal excitation of electrons near the Fermi level.[30] Thus, since the magnetic length is larger than the other lengths in our system, we feel that external field effects will be small. It is, of course, true that in the immediate proximity of the transition, where ξ becomes very large, magnetic corrections may become significant.

IV. RELAXATION PROPERTIES

If the dominant contribution to the nuclear-spin-lattice relaxation time T_1 comes from hyperfine interactions of the nuclei with conduction electrons, then the Korringa relation is valid. This relation[11] states that

$$K^2T_1T=\hbar/4\pi k(\gamma_e/\gamma_n)^2, \tag{3}$$

where K is the Knight shift, T_1 is the spin-lattice relaxation time, T is the temperature, k is Boltzmann's constant, and γ_e and γ_n are the electronic and nuclear gyromagnetic ratios. The right side of Eq. (3) is called the Korringa constant and has an invariant value for a given nuclear species.

Like KFIS, we have found that the NMR line does not relax with a single value of T_1. Rather, there is a local value of T_1 which matches a local value of the Knight shift. As noted by KFIS, this result probably arises because spin diffusion is inhibited by the differing local fields in the Knight-shift distribution. Two nuclei in different local fields cannot execute a mutual spin flip because such a flip does not conserve energy. Our homogeneous linewidth of 70 mG is much smaller than the full value of ΔH over the full concentration range of our study. Each nucleus relaxes via interactions with electrons in its own environment. Under such conditions, one might expect a local Korringa relation to be obeyed, where the local Knight shift, temperature, and local T_1 are related as noted above.

Figure 5 shows the line shape of sample A7 after four

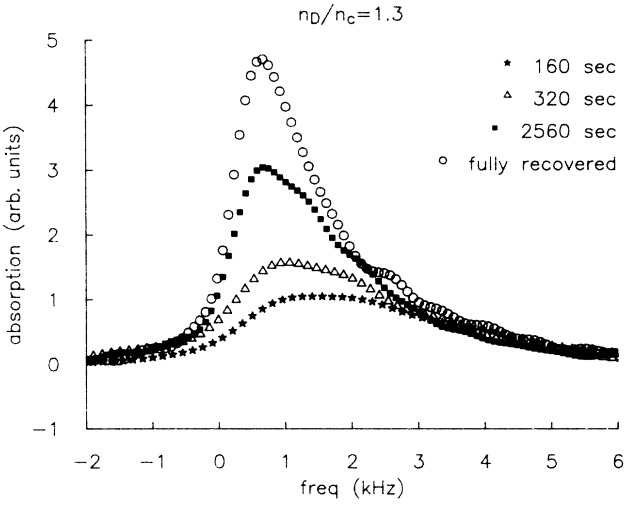

FIG. 5. Line shape for the ^{29}Si resonance in Si:As, sample A7, as a function of recovery time following a saturating comb of 90° pulses. The line shape given is the Fourier transform of the FID which follows a 90° sampling pulse applied at the times shown in the figure.

different relaxation intervals. The portions of the line with larger Knight shifts (on the right-hand side of the line in Fig. 5) are clearly relaxing faster than the portions toward the left with smaller Knight shifts. Assuming the line shape is fully relaxed after two hours (an overnight relaxation produced the same line shape), one can use the other three curves at different relaxation times to compute a rough value of T_1 at a given Knight shift. The three values of absorption amplitude for each value of Knight shift do not lie on a straight line when plotted on semilog paper, thus indicating nonexponential relaxation. We drew a smooth curve through the points and defined T_1 as the time to reach $1-1/e$ of the saturation magnetization. The values of T_1 so obtained at given values of K do follow a relationship, $K^2T_1T\simeq$const. The value of the constant is about $\frac{1}{4}$ of the Korringa constant for ^{29}Si at 4.3 K, given in Eq. (3) above. Relaxation behavior similar to that displayed in Fig. 5 was also observed in sample A2, with $n_D=0.44n_c$. However, for sample A2, a quantitative analysis showed the value of the Korringa product [Eq. (3)] to decrease near $K=0$. It may be that in this sample we are observing the onset of nuclear-spin diffusion as an energy-transfer mechanism. Spin diffusion short circuits the local Korringa mechanism for those nuclei in regions with values of K sufficiently small that mutual nuclear-spin flips are not forbidden by a gradient in K. For sample A1, at $n_{As}=1.6\times10^{18}$ cm^{-3}, the line appears to relax homogeneously.

The reduced value of the Korringa product in sample A2 could also arise from the enhanced relaxation in highly disordered systems discussed by Warren[31] and by Götze and Ketterle.[32] However, for Si:As, σ drops below the Mott minimum metallic conductivity $\sigma_{\min}$ near 8×10^{18} cm^{-3} (at 4.2 K), and one would have expected the Warren effect to make its appearance in samples with higher concentration than that of A2. It is possible that the key re-

lation of the Warren-Götze-Ketterle model embodied in Eqs. (2) and (3) of Ref. 32 is not appropriately applied to a very locally inhomogeneous system such as the doped semiconductors.

It is notable that measurable local Knight shifts and local relaxation behavior resembling those expected from the Korringa model occur in samples well below the carrier localization transition at n_c. Even though there is some thermal activation of carriers above the mobility edge in our samples at 4.3 K when n_D is just below n_c, the Korringa-like effects extend down to values $n_D = 0.44 n_c$, at which point carrier activation of 4.3 K is negligible.[33] Evidently, a local density of states is sufficiently well developed to sustain a Korringa-like relaxation.

Values of the Korringa product on both ends of our concentration range which have been obtained by previous workers[7,12,34] vary widely. Since the values were obtained by different methods in different experiments and appear to show some inconsistencies with one another, we do not believe that an attempt to understand the concentration dependence of the Korringa product is likely to be profitable.

V. SUMMARY

In the large picture, we provide no major revision of the interpretations of KFIS. Our new measurements of K and ΔH for the ^{29}Si spin system on the insulating side of the M-I transition in Si:P and Si:As show that the NMR consequences of the hyperfine interaction evolve in a continuous fashion through the transition. Measurable Knight-shift distributions, as well as a reasonable approximation to Korringa-type spin relaxation, exist for all samples with $n_D > 0.4 n_c$.

We note that satisfactory, quantitative models to explain the behavior of $\chi_s(n_D,T,H)$ and $K_i(n_D,T,H)$ in the concentration range with $n_D \gtrsim n_c$ do not yet exist. The small inconsistency of our results with those of KFIS for values for K_{pk} in Si:P at $H_0 = 9.1$ kG needs to be resolved, and we hope to do so in the near future.

ACKNOWLEDGMENTS

P. F. Newman played a major role in the design and construction of our NMR spectrometer. A. Stadnick also assisted in its construction. Conversations with R. M. Cotts and T. J. Gramila were valuable. Mohan Namboodiri assisted in determination of arsenic concentrations in samples A9 and A8, with the assistance of the staff of the Ward Reactor Laboratory. Data analysis depended heavily on computer programs developed in the Cornell University Low Temperature Group. Use of several central technical facilities supported by the Cornell University Materials Science Center through National Science Foundation Grant No. DMR-82-17227 was important to us. Major support of this work came from the National Science Foundation through Grant No. DMR-83-18511.

APPENDIX: ANALYSIS OF BACKGROUND LINEWIDTH

It became clear in the earlier NMR work in heavily doped Si[7,34] that a distribution of values of the Knight shift was an important source of inhomogeneous broadening of the ^{29}Si NMR absorption line. In order to quantitatively analyze this inhomogeneous broadening, we need to know the irreducible homogeneous width, which would presumably rise from the dipole-dipole interactions within the ^{29}Si spin system.

We measured the homogeneous linewidth for two samples, A1 and A7, by recording the height of a spin echo as a function of τ, in a standard 90°-τ-180° pulse sequence. In both samples, the decay of the spin echo with increasing τ was exponential, indicating a Lorentzian line shape. The values of the $1/e$ decay times were 5.4 ± 0.2 msec for A7 and 5.9 ± 0.4 msec for A1, equal within experimental error. We take the value of the homogeneous spin-spin relaxation time T_2 to be 5.6 msec. With a Lorentzian line shape, this value of T_2 corresponds to a full width at half maximum (FWHM) of 70 mG. We wish to compare this value with a calculated linewidth based on the ^{29}Si-^{29}Si dipolar coupling. A calculation of the expected linewidth due to the dipolar coupling can be done using the Van Vleck method of moments[35] as outlined by Abragam.[36] The second moment of the line shape due to coupling between like spins in a powdered sample is

$$M_2 = \tfrac{3}{5}\hbar^2\gamma^4 I(I+1) f \sum_i 1/r_i^6 . \tag{A1}$$

Here, γ is the gyromagnetic ratio, I is the spin of the nucleus, and r_i is the distance from a reference site to the ith nuclear site. f is the fraction of lattice sites occupied by the spins and is equal to 0.047 for the ^{29}Si isotope. The sum runs over all lattice sites. We have calculated this sum for a diamond lattice, including terms through the 13th nearest-neighbor sites and using a continuum approximation for sites beyond that. The result is

$$\sum_i 1/r_i^6 = 774/a^6 ,$$

where a is the lattice constant, 5.43 Å in silicon. The value of the second moment calculated from Eq. (A1) is $M_2 = 5.63 \times 10^5$ (rad/sec)^2.

The shape of the NMR absorption line can be characterized by forming the ratio of the fourth moment to the square of the second moment, $M_4/(M_2)^2$. The general expression for the nth moment is $M_n = \int \omega^n f(\omega) d\omega$, where $f(\omega)$ is the line-shape function. If the line shape has a Gaussian form, $M_4/(M_2)^2$ has a value of 3. For a line shape with longer tails, such as a Lorentzian, the ratio increases. For a true Lorentzian line, the integrals which define the even numbered moments diverge and the value of the ratio becomes indeterminate.

A value for the fourth moment has not been calculated for the diamond lattice. However, we can make some progress by using the expression for the ratio $M_4/(M_2)^2$ which was worked out for a simple cubic lattice by Kittel and Abrahams,[37] for a external magnetic field oriented along the [100] direction. Their expression is

$$M_4/(M_2)^2=3\{0.74+[0.098-0.021/I(I+1)]/f\} .$$

One sees that for $f=1$, corresponding to a completely filled cubic lattice, the ratio $M_4/(M_2)^2$ is equal to 2.4, indicating a line shape resembling a Gaussian. However, in a magnetically dilute system with $f\ll 1$, the ratio $M_4/(M_2)^2$ can become very large, signaling the approach to a Lorentzian line shape. For the ^{29}Si spin system, with $f=0.047$, the cubic lattice approximation gives $M_4/(M_2)^2=6.7$. This cubic lattice value probably underestimates the value of the moment ratio for a diamond lattice. The diamond structure is not as compact as a cubic structure, the number of nearest neighbors being four instead of six. Hence, for a given value of f, a lattice point in the diamond structure has a lower probability of having a nearest neighbor than in the simple cubic structure. Because the nearest neighbors dominate the other lattice points in the calculation of the moments, the ratio $M_4/(M_2)^2$ in a diamond lattice with a given f will be equal to the ratio in a simple cubic lattice with a smaller f.

We consider the Lorentzian line-shape function with a halfwidth at half maximum of δ. Thus,

$$f(\omega)=(\delta/\pi)[1/(\delta^2+\omega^2)] .$$

The even moments of a true Lorentizan do not exist. However, one can make useful progress by cutting off the defining moment integrals at a value $|\omega|=\alpha$ which is much larger than δ. Then, using the equation $M_n=\int_{-\alpha}^{\alpha}\omega^n f(\omega)d\omega$, we obtain the approximate relations, neglecting terms of order δ/α,

$$M_2=\frac{2\alpha\delta}{\pi}, \quad \frac{M_4}{(M_2)^2}=\frac{\pi\alpha}{6\delta} ,$$

and thus,

$$\delta=\frac{\pi}{2\sqrt{3}}\left[\frac{(M_2)^2}{M_4}\right]^{1/2}(M_2)^{1/2} . \tag{A2}$$

One notes that the condition $\alpha\gg\delta$ is equivalent to the condition

$$(6/\pi)[M_4/(M_2)^2]\gg 1 .$$

This quantity, for the ^{29}Si system, was estimated to be at least as large as $(6/\pi)6.7=12.8$. Thus, it seems reasonable to approximate the ^{29}Si dipolar line shape by a Lorentzian.

Using Eq. (A2), with the calculated value of 5.63×10^5 (rad/sec)^2 for M_2 and the approximation $M_4/(M_2)^2=6.7$, leads to a predicted FHWM of 526 rad/sec. We can convert this to an equivalent spread in local magnetic fields with the standard relation $\Delta\omega=\gamma\Delta H$ yielding a value of 100 mG for the predicted value of FWHM.

This value of 100 mG, given the approximations used in arriving at it, seems to good agreement with the measured homogeneous width of 70 mG. Thus, we believe that the 70-mG homogeneous width arises from the ^{29}Si-^{29}Si dipole interaction.

As mentioned, the linewidths of our lowest concentration samples P1 and A1 are inhomogeneously broadened to widths of about half a gauss. While we are not certain of the source of this broadening, there are some causes that we can rule out. The effect of inhomogeneities in internal fields arising from random demagnetizing factors associated with the irregularly shaped sample particles has been calculated by Drain.[38] We find that the field spread can be approximated by

$$\Delta H=3\chi H_0 ,$$

where χ is the total static magnetic susceptibility and H_0 is the applied field. Silicon has a core diamagnetic susceptibility, $\chi=-1.2\times10^{-7}$ emu/g.[39] The susceptibility of the donor electrons varies with concentration but is of the order of 5×10^{-8} emu/g, as can be seen from the susceptibility data of Quirt and Marko in Fig. 2. The total χ is the sum of these. A conservative assumption gives $|\chi|=1\times10^{-7}$ emu/g. With an applied field of 60 kG, conversion of χ to dimensionless form yields a value for ΔH of 40 mG, much smaller than the observed linewidth.

Dipolar interactions between nuclei and localized electronic moments also appear to be too weak to cause the observed line broadening. We can estimate a typical distance from a silicon nucleus to an impurity site using Poisson statistics. At any given site in the silicon lattice, the probability of finding no impurity within a distance r is $\exp[-(4\pi n_D r^3/3)]$. We define the typical impurity separation to be the distance which gives the above probability a value of $\frac{1}{2}$. This yields $r=0.55n^{-1/3}$. For sample P1, with $n_D=1.1\times10^{17}$ cm^{-3}, this typical impurity separation is 115 Å. The magnetic field from a dipole with the strength of 1 Bohr magneton at a distance of 115 Å is $\mu_B/r^3=6$ mG. Again, this is too small an effect to be the cause of the 500-mG broadening observed.

[1]T. F. Rosenbaum, R. F. Milligan, M. A. Paalanen, G. A. Thomas, R. N. Bhatt, W. Lin, Phys. Rev. B **27**, 7509 (1983).

[2]P. F. Newman and D. F. Holcomb, Phys. Rev. B **28**, 638 (1983).

[3]W. N. Shafarman, T. G. Castner, J. S. Brooks, K. P. Martin, and M. J. Naughton, Solid State Electron. **28**, 93 (1985).

[4]K. Andres, R. N. Bhatt, P. Goalwin, T. M. Rice, and R. E. Walstedt, Phys. Rev. B **24**, 244 (1981).

[5]R. N. Bhatt and P. A. Lee, Phys. Rev. Lett. **48**, 344 (1982).

[6]J. D. Quirt and J. R. Marko, Phys. Rev. B **7**, 3842 (1973).

[7]R. K. Sundfors and D. F. Holcomb, Phys. Rev. **136**, A810 (1964).

[8]Shun-ichi Kobayashi, Yoichi Fukagawa, Seiichiro Ikehata, and Wataru Sasaki, J. Phys. Soc. Jpn. **45**, 1276 (1978).

[9]T. G. Castner, N. K. Lee, G. S. Cieloszyk, and G. L. Salinger, Phys. Rev. Lett. **34**, 1627 (1975).

[10]Harold F. Hess, Keith DeConde, T. F. Rosenbaum, and G. A. Thomas, Phys. Rev. B **25**, 5578 (1982).

[11]J. Korringa, Physica **16**, 601 (1950).

[12]D. Jerome, C. Ryter, and J. M. Winter, Physics **2**, 81 (1965).

[13]D. Jerome, C. Ryter, H. J. Schulz, and J. Friedel, Philos. Mag. B **52**, 403 (1985).

[14]M. A. Dubson, Ph.D. thesis, Cornell University, 1984.
[15]M. A. Paalanen, A. E. Ruckenstein, and G. A. Thomas, Phys. Rev. Lett. **54**, 1295 (1985).
[16]G. C. Brown and D. F. Holcomb, Phys. Rev. B **10**, 3394 (1974).
[17]W. R. Thurber, R. L. Mattis, Y. M. Liu, and J. J. Filliben, J. Electrochem. Soc. **127**, 1807 (1980).
[18]P. F. Newman, M. J. Hirsch, and D. F. Holcomb, J. Appl. Phys. **58**, 3779 (1985).
[19]M. I. Gordon, Ph.D. thesis, University of Natal, South Africa, 1977.
[20]J. D. Ellett, M. G. Gibby, V. Haeberlen, L. M. Huber, M. Mehring, A. Pines, and J. S. Waugh, Adv. Magn. Reson. **5**, 117 (1971).
[21]It is also possible, by using a digital oscilloscope and Fourier-transform routines, to filter the FID digitally. This technique eliminates any distortion in the Fourier transform caused by the roll-off characteristic and phase response of a conventional analog audio filter.
[22]J. D. Quirt and J. R. Marko, Phys. Rev. B **5**, 1716 (1972).
[23]A. P. Long and M. Pepper, J. Phys. C **17**, L425 (1984).
[24]S. Maekawa and N. Kinoshita, J. Phys. Soc. Jpn. **20**, 1447 (1965).
[25]R. L. Aggarwal and A. K. Ramdas, Phys. Rev. **140**, A1246 (1965).
[26]P. R. Cullis and J. R. Marko, Phys. Rev. B **1**, 632 (1970).
[27]D. P. Tunstall and V. G. I. Deshmukh, J. Phys. C **12**, 2295 (1979).
[28]N. F. Mott, Philos. Mag. **6**, 287 (1961).
[29]B. I. Shklovskii and A. L. Efros, *Electronic Properties of Doped Semiconductors* (Springer-Verlag, Berlin, 1984), pp. 43–45.
[30]Y. Imry, J. Appl. Phys. **52**, 1817 (1981).
[31]W. W. Warren, Jr., Phys. Rev. B **3**, 3708 (1971).
[32]W. Götze and W. Ketterle, Z. Phys. B **54**, 49 (1983).
[33]C. Yamanouchi, K. Mizuguchi, and W. Sasaki, J. Phys. Soc. Jpn. **22**, 859 (1967).
[34]W. Sasaki, S. Ikehata, and S. Kobayashi, J. Phys. Soc. Jpn. **36**, 1377 (1974).
[35]J. H. Van Vleck, Phys. Rev. **74**, 1168 (1948).
[36]A. Abragam, *The Principles of Nuclear Magnetism* (Oxford University Press, London, 1961), Chap. IV.
[37]C. Kittel and E. Abrahams, Phys. Rev. **90**, 238 (1953).
[38]L. E. Drain, Proc. Phys. Soc. London **80**, 1380 (1962).
[39]E. Sonder and D. K. Stevens, Phys. Rev. **110**, 1027 (1958).